Photoionization studies of the $2p$ resonances of atomic calcium

B. Obst,[1] J. E. Hansen,[2] B. Sonntag,[3] Ph. Wernet,[3] and P. Zimmermann[1,*]
[1]*Institut für Atomare und Analytische Physik, Technische Universität Berlin, Hardenbergstrasse 36, D-10623 Berlin, Germany*
[2]*Department of Physics and Astronomy, University of Amsterdam, Valckenierstraat 65, NL-1018 XE Amsterdam, Netherlands*
[3]*II. Institut für Experimentalphysik, Universität Hamburg, Luruper Chaussee 149, D-22761 Hamburg, Germany*
(Received 9 July 2001; published 18 June 2002)

The Ca $2p$ resonances at 345–355 eV were studied by photoion and photoelectron spectroscopy using monochromatized synchrotron radiation and atomic-beam technique. The analysis of the excitation and decay of these resonances shows strong configuration mixing between the different subshells of the valence electrons $4s$, $3d$, and $4p$. In the case of the $2p_{3/2}^{-1}$ resonance structure at 348 eV there are two excited states with nearly equal contributions from the configuration $2p^5 3d 4s^2$ and $2p^5 3d^2 4s$, which gives rise to strong variations of the resonantly enhanced $3p^4(3d,4s)^3$ photoelectron lines when scanning the photon energy across the resonance.

DOI: 10.1103/PhysRevA.65.062716 PACS number(s): 32.80.Fb, 32.80.Hd

I. INTRODUCTION

The photoionization cross section of the atomic ground state of Ca $(1s^2 2s^2 2p^6 3s^2 3p^6 4s^2\ ^1S_0)$ shows strong resonances below the $3p^{-1}$ as well as the $2p^{-1}$ thresholds. These resonances can be attributed to discrete transitions $np^6 4s^2 \rightarrow np^5(3d,4s)^3$. The notation $np^5(3d,4s)^3$ implies that due to the near degeneracy of the $3d$ and $4s$ orbitals in the presence of a np^{-1} core hole, there is strong mixing between the $3d4s^2$, $3d^2 4s$, and $3d^3$ configurations. A detailed theoretical analysis reveals that even other configurations, such as $3d4p^2$ mix in strongly. This results in a complex situation for the analysis of these resonances.

The $3p$ resonances in the photon-energy region from 20 eV to 40 eV have been extensively studied by many experimental and theoretical investigations (see [1,2] and references therein). For the deep innershell $2p$ resonances, however, only a few investigations exist [3–8]. They are based on absorption [3], ion-yield [4,5], and photoelectron studies [6–8]. In order to gain insight into the configuration mixing in the $2p$ resonances we performed ion-yield and photoelectron studies with considerably improved experimental photon- and electron-energy resolution. The high-resolution spectra in return triggered calculations so we can present experimental as well as theoretical results on the $2p$ resonances of atomic calcium.

II. EXPERIMENTAL SETUP

The experimental investigations were carried out at the undulator beamline BW3 of the synchrotron radiation facility HASYLAB in Hamburg (Germany). The synchrotron radiation was monochromatized by a SX700 monochromator and crossed at a right angle with a collimated atomic Ca beam.

The photon bandwidth of the monochromator was 140 meV for measurements of the electron spectra and 240 meV for the ion-yield spectra. Ca was vaporized in a resistively heated steel crucible at temperatures around 850 °K. A separately heated nozzle was used to collimate the atomic beam. The region of interaction was surrounded by two concentric μ-metal cylinders. The common axis of these μ-metal shieldings was oriented at the magic angle of 54 °44″ with respect to the main axis of the polarization ellipse of the light.

The kinetic energy of electrons emitted along the symmetry axis of the μ-metal shielding was analyzed by a SCIENTA SES200 hemispherical electron spectrometer. The different electron spectra shown were recorded at a pass energy of 75 eV with a resolution of $\Delta E = 140$ meV. The photoions were detected by a conventional two-stage Wiley-McLaren-type time-of-flight spectrometer.

Utilizing the linearity and calibration of the relative energy scale of the electron analyser, the absolute energy scales of the monochromator and the electron analyser were calibrated by measuring photo and Auger lines of noble gases for several photon energies around 350 eV. The photoelectron as well as the ion-yield spectra were corrected for changes in the photon flux density during the measurements.

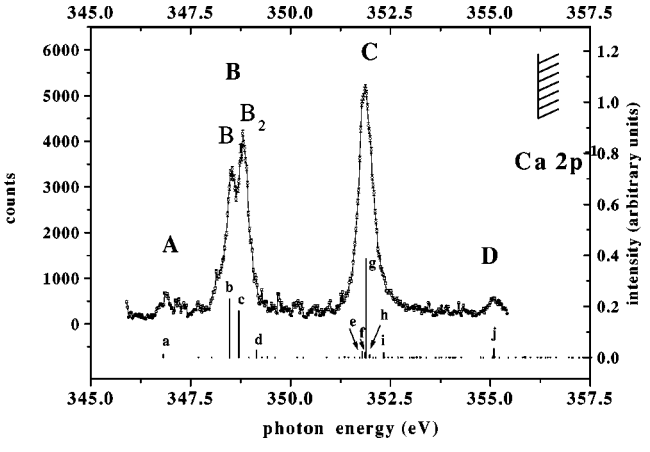

FIG. 1. Total ion-yield spectrum of atomic Ca showing the $2p$ resonances. The scatter of the data points indicates the experimental uncertainties. The statistical uncertainties are indicated by the error bars. The stick diagram gives the calculated transition probabilities to the various $2p$ core excited resonances.

*Author to whom correspondence should be addressed.

TABLE I. List of configurations included in the Hartree-Fock-calculations for the initial, resonance, and final states.

No.	Initial state Ca I	Resonance state Ca* I	Final state Ca II
1	$3p^6 4s^2$	$2p^5 3d 4s^2$	$3s^2 3p^4 3d 4s^2$
2	$3p^6 4p^2$	$2p^5 4s^2 4d$	$3s^2 3p^4 4s^2 4d$
3	$3p^6 3d^2$	$2p^5 3d 4p^2$	$3s^2 3p^4 4s^2 5d$
4	$3p^6 4d^2$	$2p^5 4p^2 4d$	$3s^2 3p^4 4s^2 6d$
5	$3p^6 5s^2$	$2p^5 4s 4p^2$	$3s^2 3p^4 4s^2 7d$
6		$2p^5 3d^3$	$3s^1 3p^6 4s^2$
7		$2p^5 3d^2 4s$	$3s^1 3p^6 4p^2$
8			$3s^1 3p^6 3d^2$
9			$3s^1 3p^6 3d 4s$
10			$3s^2 3p^4 3d 4p^2$
11			$3s^2 3p^4 4p^2 4d$
12			$3s^2 3p^4 3d^2 4s$
13			$3s^2 3p^4 4s 4d^2$
14			$3s^2 3p^4 3d^3$
15			$3s^2 3p^5 4s 4p$

The photoelectron spectra were also corrected for the kinetic-energy-dependent transmission of the electron analyzer. The transmission curve was determined in a procedure analogous to the one described by Jauhiainen *et al.* [9].

III. RESULTS

A. The excitation of the Ca 2*p* resonances

Figure 1 shows the ion-yield spectrum of atomic Ca in the region of the $2p$ resonances between 345 eV and 355 eV. Also the first ionization threshold of the direct $2p$ ionization is marked in this figure [10]. There are two dominant resonances: B at 348.7 ± 0.2 eV and C at 351.8 ± 0.2 eV. Furthermore, there are two weaker resonances: A at 347 ± 0.2 eV and D at 355 ± 0.2 eV. The distance between the dominating resonances B and C corresponds to the spin-orbit splitting of the $2p$ hole. Therefore, they can be labeled by $2p_{3/2}^{-1}$ (B) and $2p_{1/2}^{-1}$ (C) as they were already identified and assigned by Mansfield [3]. A closer look at the resonances B and C, however, reveals that the situation is more complex. The resonance B consists of at least two resonances: B_1 at 348.5 eV and B_2 at 348.8 eV. Furthermore there is a shoulder at the low-energy side of the resonance B_1, and for resonance C there is a shoulder at the high-energy side indicating that also this resonance consists of several lines. Obviously the interaction of the $2p$ hole with the three valence electrons cannot be described by the single configuration $3d4s^2$, which only accounts for two $2p_{3/2}^{-1} 3d4s^2$ resonances, the dominant resonance B and the much weaker resonance A at 347 ± 0.2 eV.

For a better understanding of the $2p$ resonance structure we performed Hartree-Fock calculations for the absorption spectrum incorporating configuration mixing between the valence subshells $3d$, $4s$, $4p$, $4d$, and $5s$. Table I lists, in the second and third rows, the sets of configurations used in the ground state and the excited states in these calculations. The results are depicted on the bottom of Fig. 1. Instead of the expected three lines for the transition $2p^6 4s^2 \rightarrow 2p^5 3d 4s^2$, now a large number of lines show up for which the strongest ones are labeled by $a, b, \ldots, j$. The comparison with the ion-yield spectrum shows that the main resonance structure

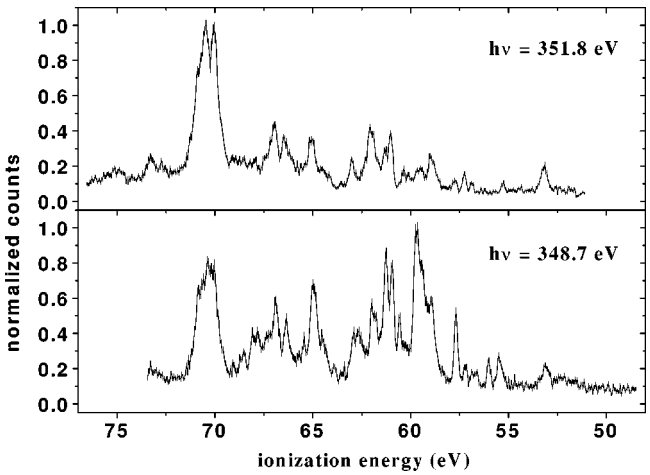

FIG. 2. Photoelectron spectra of resonantly excited atomic Ca. Top: Decay of the $2p_{1/2}^{-1}$ (C) resonance, excited at $h\nu = 351.8$ eV, into $Ca^+ 3p^{-2}$ and $3s^{-1}$ states. Bottom: Decay of the $2p_{3/2}^{-1}$ (B) resonance, excited at $h\nu = 348.7$ eV, into $Ca^+ 3p^{-2}$ and $3s^{-1}$ states. In each spectrum the amplitude of the strongest line is set equal to 1.0.

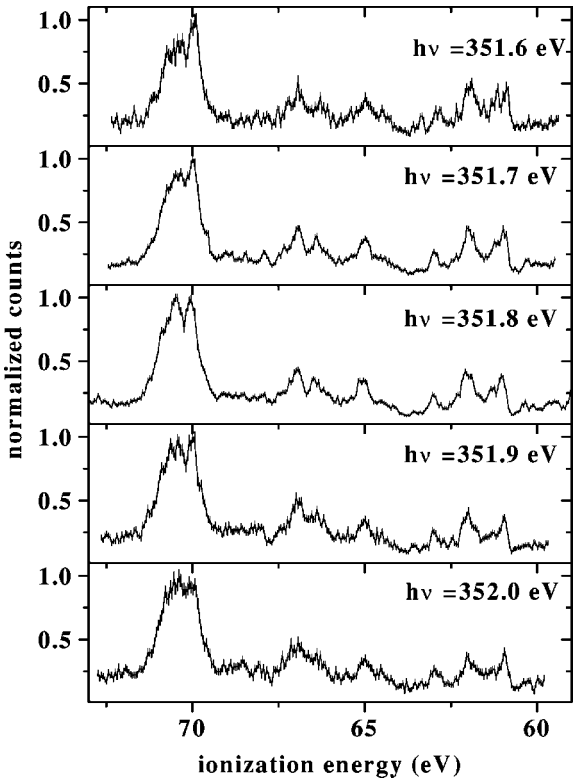

FIG. 3. $Ca^+ 3p^{-2}$ and $3s^{-1}$ photoelectron spectra in the range of the $2p_{1/2}^{-1}$ resonance (C). The photon energy is increased in steps of 0.1 eV from 351.6 eV (top) to 352.0 eV (bottom). In each spectrum the amplitude of the strongest line is set equal to 1.0.

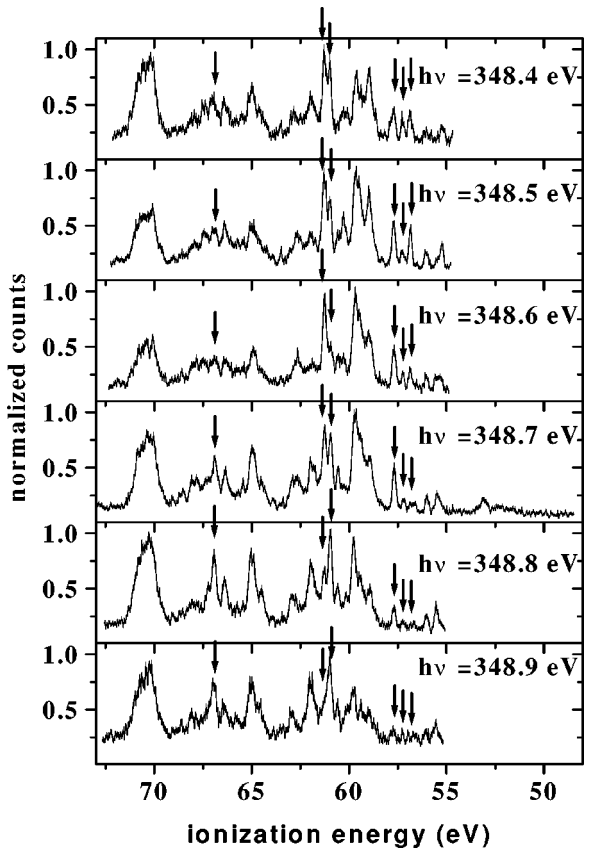

FIG. 4. $Ca^+ 3p^{-2}$ and $3s^{-1}$ photoelectron spectra in the range of the $2p_{3/2}^{-1}$ resonance (B). The photon energy is increased in steps of 0.1 eV from 348.4 eV (top) to 348.9 eV (bottom). The arrows mark regions of drastic changes in line intensities as the photon energy is varied (see text). In each spectrum the amplitude of the strongest line is set equal to 1.0.

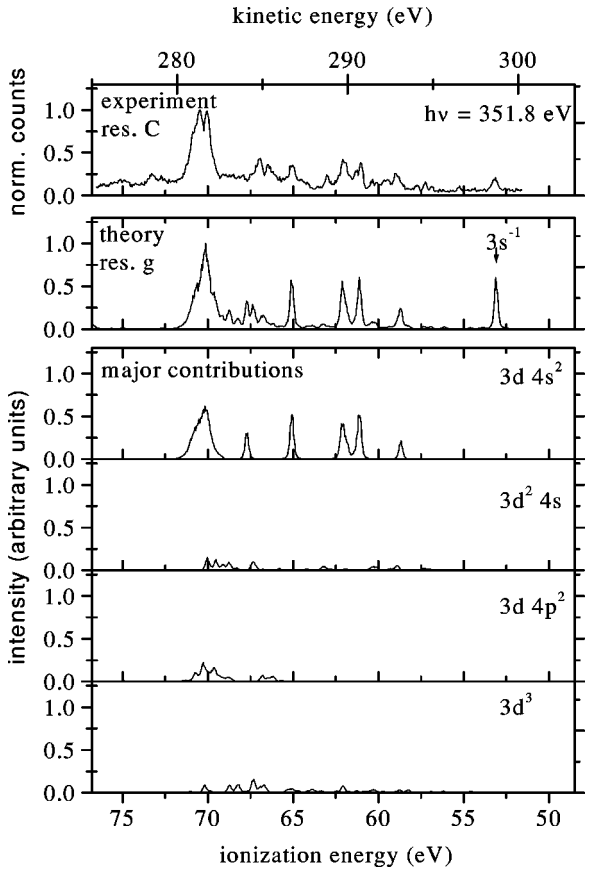

FIG. 5. Comparison of the experimental photoelectron spectrum of the $2p_{1/2}^{-1}$ (C) resonance recorded at $h\nu=351.8$ eV with a theoretical spectrum for resonance g. The lower four graphs show the individual contributions to the theoretical spectrum from the four most important configurations involved in the final-state mixing.

is well reproduced: Resonance C is represented by the strong line g and several much weaker lines e, f, h, and i, resonance B by two strong lines b and c and a weaker line d, resonances A and D by the weak lines a and j. On the other hand the agreement is not perfect. For example, the order of the lines b, c, and d should be reversed to produce the structure of resonance B. However, we note that the calculated spectrum is sensitive to the scaling factors used for the Slater integrals. Therefore, it is difficult to give definite assignments for all the resonances. Also there is strong configuration mixing in the $2p$ core excited state, which does not allow the association of one configuration to each excited state. Nevertheless one can make the following assignments for the main contributions: For resonance C the main contribution g is due to the configuration $3d4s^2$, for resonance B the main contributions b and c are both due to the mixed configurations $3d4s^2$ and $3d^24s$. The smaller resonance A and D are due to the configurations $3d4s^2$ (A) and $4d4s^2$ (D).

For further insight into the resonance structure we studied the electronic decay of the resonances, which will be described in the following section.

B. Electronic decay of the Ca 2*p* resonances

The electronic decay of the Ca $2p$ resonances was already extensively studied by Meyer *et al.* [6,7] both experimentally and theoretically. For the dominant decay channel $Ca\ 2p^{-1} \rightarrow Ca^+\ 3p^{-2}$ at binding energies between 55–75 eV they found a striking difference in the photoelectron spectra between the main resonances $2p_{3/2}^{-1}$ (B) ($h\nu=348$ eV; $\Delta h\nu=0.6$ eV) and $2p_{1/2}^{-1}$ (C) ($h\nu=352$ eV; $\Delta h\nu=0.6$ eV). Their calculations of the electron spectra incorporated configuration mixing in the resonant atomic states $2p^{-1}(3d4s^2+3d4p^2+3d^24s+3d^3)$ and final ionic states $3p^{-2}(3d4s^2+3d4p^2+3d^24s+3d^3)$. The qualitative differences between the decays of the two peaks were reproduced but not all the details of the electron spectra. Matsuo *et al.* [5] observed a broadening of peak B and suggested that this peak contained additional structure, which was confirmed by Obst *et al.* [8]. This observation makes it worthwhile to extend the earlier work.

Figure 2 shows the photoelectron spectra of the two resonances B and C recorded with improved experimental conditions by using an advanced high-resolution electron spectrometer as well as a high-resolution monochromator. The upper part of Fig. 2 presents the decay of the resonance $2p_{1/2}^{-1}$ (C) taken at $h\nu=351.8$ eV, the lower part that of resonance $2p_{3/2}^{-1}$ (B) taken at $h\nu=348.7$ eV. One observes a rather dense spectrum of which at first sight altogether 38 lines can be identified (for a table of ionization energies see

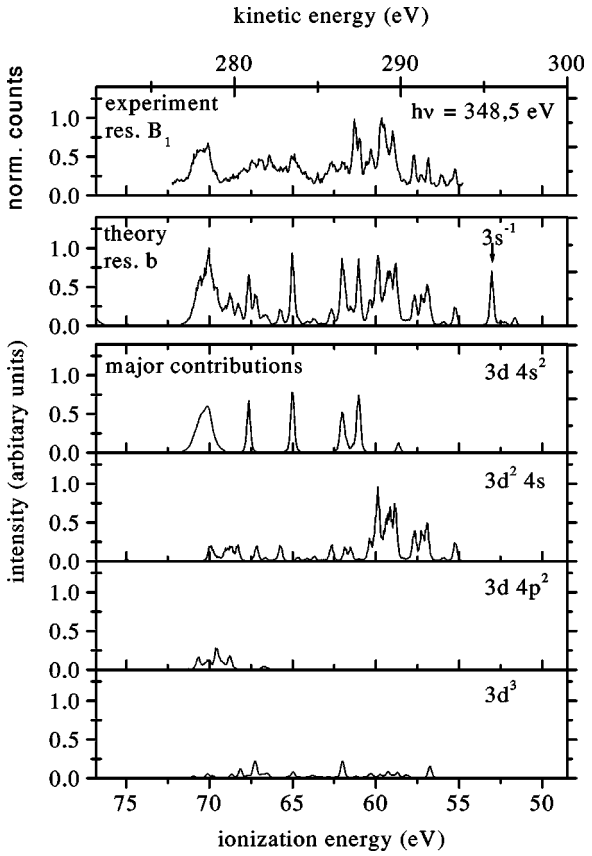

FIG. 6. Comparison of the experimental photoelectron spectrum of the $2p_{3/2}^{-1}$ (B_1) resonance recorded at $h\nu=348.5$ eV with a theoretical spectrum for resonance *b*. The lower four graphs show the individual contributions to the theoretical spectrum from the four most important configurations involved in the final-state mixing.

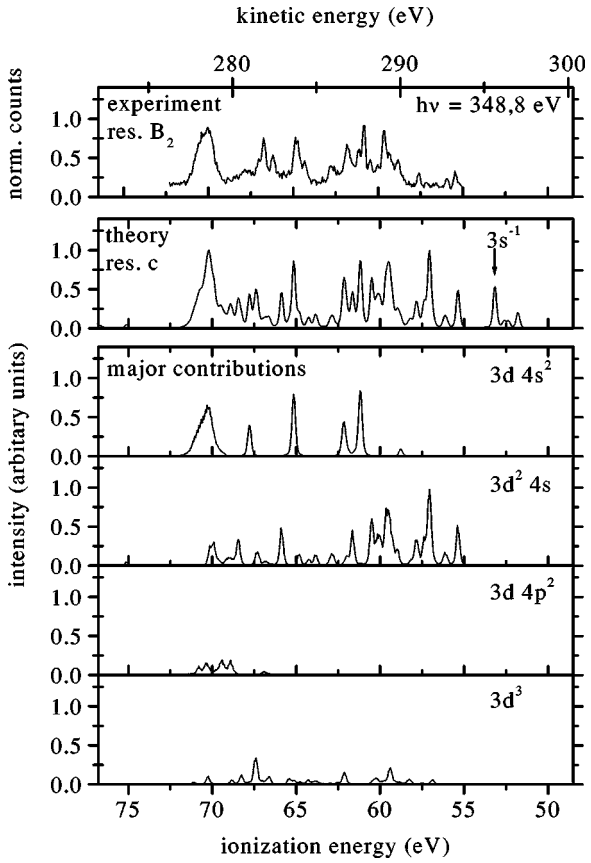

FIG. 7. Comparison of the experimental photoelectron spectrum of the $2p_{3/2}^{-1}$ (B_2) resonance recorded at $h\nu=348.8$ eV with a theoretical spectrum for resonance *c*. The lower four graphs show the individual contributions to the theoretical spectrum from the four most important configurations involved in the final-state mixing.

[11]). Eleven of these lines obviously are common to both resonances. The line at 53.1 eV is due to the $3s$ ionization. The overall structure is consistent with the low-resolution spectra of Meyer *et al.* [6,7].

From the analysis of the ion-yield spectrum we know that both resonances $2p_{3/2}^{-1}$ (B) and $2p_{1/2}^{-1}$ (C) have a complex structure caused by contributions of different configurations. In order to shed light on the energy dependence of the excited-state configuration mixing we made use of the improved experimental resolution and scanned the photon energy in steps of 100 meV across both resonances while keeping the monochromator bandwidth of 150 meV fixed. In Figs. 3 and 4 the corresponding photoelectron spectra are depicted. The study of the series of photoelectron spectra reveals that apart from the difference in the spectra taken at resonances *B* and *C*, there are also marked differences for the much smaller variations of the photon energy in this case. Whereas for resonance *C* the relative line intensities in the spectra are nearly constant (Fig. 3), in the case of resonance *B* there are drastic changes in the individual line intensities (marked by arrows in Fig. 4).

This behavior agrees with the results of Sec. III A that resonance *B* consist of at least two excited states and that the difference between resonance *B* and *C* originates in the different contributions of the valence electron configurations (essentially $3d4s^2$ and $3d^24s$). To compare these results with theoretical electron spectra we performed Hartree-Fock calculations in the same way as in previous studies of Meyer *et al.* [6,7] but with an increased basis set of configurations. In the fourth row of Table I the configurations of the final ionic states are listed. The theoretical electron spectra are shown in Figs. 5, 6, and 7 together with the experimental spectra taken at the resonances C, B_1, and B_2. The theoretical spectra are based on the calculated decay probabilities of the main resonances b (B_1), c (B_2), and g (C) into the numerous Ca^+ $3p^{-2}$ and $3s^{-1}$ final states giving rise to the multiline photoelectron spectra displayed in Figs. 5, 6, and 7. In the experimental and the theoretical spectrum the amplitude of the most intense structure was set to 1.0. Below the theoretical spectra the major contribution from the different configurations of the valence electrons $3d4s^2$, $3d^24s$, $3d4p^2$, and $3d^3$ are given. These spectra are scaled (in intensity and energy) identically to the theoretical sum spectrum. For the resonant photoelectron spectra the width of the lines is determined by the instrumental resolution and the lifetime of the final ionic states. From single configuration calculations for the lifetimes of the Ca^+ $3p^4 3d4s^2$ multiplet components it is known [7] that the Ca^+ $3p^4(^3P)3d4s^2\,^2D$, and ^2P terms have a width of 0.5–0.6 eV while all other components have widths less than 0.1 eV. Therefore, all lines

TABLE II. Results of the Hartree-Fock-calculations. In the top section the relative positions and the total decay probabilities for the three major resonance states $b\,(B_1)$, $c\,(B_2)$, and $g\,(C)$ are given. In the lower part the relative decay intensities into states of the different final-state configurations are shown. Configurations marked ''−'' did not contribute any lines with a decay probability of $1.0\times10^{9}\ s^{-1}$ or greater.

		$b\,(B_1)$	$c\,(B_2)$	$g\,(C)$
Rel. position (eV)		−0.786	−0.556	2.637
Total decay probability (s)		1.36×10^{14}	1.35×10^{14}	1.41×10^{14}
No.	Configuration	%	%	%
	All (sum) [a]	100.00	100.00	100.00
1	$3s^23p^43d4s^2$	34.37	29.89	52.83
2	$3s^23p^44s^24d$	0.98	0.78	1.32
3	$3s^23p^44s^25d$	0.48	0.38	0.71
4	$3s^23p^44s^26d$	0.13	0.10	0.21
5	$3s^23p^44s^27d$	0.06	0.04	0.10
6	$3s^13p^64s^2$	4.03	3.19	6.51
7	$3s^13p^64p^2$	0.02	0.02	0.21
8	$3s^13p^63d^2$	0.23	0.24	0.53
9	$3s^13p^63d4s$	1.42	3.29	0.35
10	$3s^23p^43d4p^2$	7.92	7.62	12.04
11	$3s^23p^44p^24d$	−	−	0.01
12	$3s^23p^43d^24s$	41.33	43.04	12.73
13	$3s^23p^44s4d^2$	−	−	0.00
14	$3s^23p^43d^3$	8.89	11.25	12.09
15	$3s^23p^54s4p$	0.15	0.16	0.35

[a]The sum is set to 100.00. The sum over all contributions may differ due to rounding errors.

were convoluted with an estimated lifetime broadening of less than 0.1 eV except for the multiplet lines just mentioned [$Ca^+\ 3p^4(^3P)3d4s^2\,^2D$, and ^2P] for which a natural broadening of 0.5 eV was assumed. The instrumental broadening was taken into account by convoluting the theoretical bar diagram with a resultant Gaussian of 200 meV representing the monochromator bandpath (145 meV) and the electron analyzer resolution (135 meV). Table II lists the calculated decay probabilities of the three main resonances $b\,(B_1)$, $c\,(B_2)$, and $g\,(C)$ to the 15 final ionic state configurations (fourth row of Table I). The energy of the theoretical $3s^{-1}$ line was matched to the experimental value by shifting the whole calculated spectrum by 0.2 eV towards lower ionization energies. The theoretical intensity ot the $3s^{-1}$ line is too large due to the lack of correlation in the calculation as explained earlier [7].

In view of the complexity of such calculations there is a surprisingly good agreement with the experimental spectra. In Fig. 5 one notes that the spectrum is dominated by lines attributed to the configuration $3d4s^2$. These lines make up roughly 53% of the total intensity of the electron spectra. The lines belonging to the other configurations shown, each amount to a little over 12%. These results corroborate the finding that resonance C is a $2p^53d4s^2$ resonance.

On the other hand in Figs. 6 and 7 the intensity is dominated by the lines attributed to the configuration $3d^24s$. The intensity of the $3d4s^2$ lines drops for these spectra to around 34% and 30%. The difference in appearance of two spectra is mainly due to the changing relative line intensities within the configuration $3d^24s$. These changes reflect the strong interconfiguration mixing of the configurations $3d^24s$ and $3d4s^2$. It should be kept in mind that the theoretical spectra correspond to the pure decay of either of the two resonances while the experimental spectra contain an unresolved mixture of the two.

As the main result one can deduce that the detailed structure of the photoelectron spectra from Ca $2p$ resonances can only be reproduced by strong configuration mixing of the valence electrons $4s$, $3d$, and $4p$. There is a pronounced difference in the photoelectron spectra of the resonances $2p_{1/2}^{-1}$ (C) and $2p_{3/2}^{-1}$ (B). Whereas the major contributions to the electron spectra of resonance C is due to the configuration $3d4s^2$, the electron spectra of resonance B_1 and B_2 are due to nearly equal contributions of the configurations $3d4s^2$ and $3d^24s$ for both resonances.

ACKNOWLEDGMENTS

The authors express their gratitude for the support during the beam time to W. Benten, J. Costello, and A. Verweyen and for fruitful discussions to M. Meyer. This work was funded by the Deutsche Forschungsgemeinschaft. The support of the HASYLAB staff and especially of the BW3-SX700 crew is gratefully acknowledged.

[1] B. Sonntag and P. Zimmermann, Rep. Prog. Phys. **55**, 911 (1992).
[2] J. M. Bizau, P. Girard, F. J. Wuilleumier, and G. Wendin, Phys. Rev. A **36**, 1220 (1987).
[3] M. W. D. Mansfield, Proc. R. Soc. London, Ser. A **348**, 143 (1976).
[4] Y. Sato, T. Hayaishi, Y. Itikawa, Y. Itoh, J. Murakami, T. Nagata, T. Sasaki, B. Sonntag, A. Yagishita, and M. Yoshino, J. Phys. B **18**, 225 (1985).
[5] T. Matsuo, T. Hayaishi, Y. Itoh, T. Koizumi, T. Nagata, Y. Sato, E. Shigemasa, A. Yagishita, M. Yoshino, and Y. Itikawa, J. Phys. B **25**, 121 (1992).
[6] M. Meyer, E. v. Raven, M. Richter, B. Sonntag, R. D. Cowan, and J. E. Hansen, Phys. Rev. A **39**, 4319 (1989).
[7] M. Meyer, E. v. Raven, B. Sonntag, and J. E. Hansen, Phys. Rev. A **49**, 3685 (1994).
[8] B. Obst, W. Benten, A. von dem Borne, J. Costello, L. Dardis, Ch. Gerth, P. Glatzel, A. Grays, J. E. Hansen, O. Meighan, E. Kennedy, C. McGuinness, B. Sonntag, A. Verweyen, Ph. Wernet, and P. Zimmermann, J. Electron Spectrosc. Relat. Phenom. **101–103**, 39 (1999).
[9] J. Jauhiainen, A. Ausmees, A. Kivimäki, S. J. Osborne, A.

Navees de Brito, S. Aksela, S. Svensson, and H. Aksela, J. Electron Spectrosc. Relat. Phenom. **69**, 181 (1994).

[10] Ph. Wernet, P. Glatzel, A. Verweyen, B. Sonntag, B. Obst, W. Benten, Ch. Gerth, P. Zimmermann, A. Gray, and J. Costello, J. Phys. B **31**, L289 (1998).

[11] B. Obst, *Hochauflösende Photoelektronenspektroskopie an atomarem Kalzium und Scandium mit Synchrotronstrahlung im Bereich der resonanten 2p-Anregung* (Wissenschaft und Technik, Berlin, 2001).